Journal of Membrane Science, 73 (1992) 143–152
Elsevier Science Publishers B V , Amsterdam

Characterization of hollow fiber hemodialysis membranes: pore size distribution and performance*

Arnold P Broek, Herman A. Teunis, Derk Bargeman, Erik D Sprengers** and Cees A Smolders
University of Twente, Dept of Chemical Technology, P O Box 217, 7500 AE Enschede (The Netherlands)

(Received June 25, 1991, accepted in revised form April 6, 1992)

Abstract

The effect of two commonly used sterilization methods for artificial kidneys on the morphology and performance of hollow fiber Hemophan® hemodialysis membranes was studied A relatively new membrane characterization method, thermoporometry, was used to determine the pore size distributions and porosities of the differently treated membrane samples The samples used for this study were not treated with a concentrated glycerol solution before sterilization Hemophan was found to have a pore size distribution with pore radii between 1 5 and 12 nm, the volume porosity was 20% The sample sterilized with ethylene oxide (EtO) had a volume porosity of 18% which was due to a decrease of the pore volume of the smallest pores The applied dry steam sterilization treatment resulted in a drastic collapse of the large pores while smaller pores were formed The calculated porosity was only 10% The 'tortuous capillary pore model' was used to predict the performance of the artificial kidneys from the pore size distribution in the membrane material *In vitro* dialysis experiments with creatinine and vitamin B12 were carried out to compare the calculated and measured clearance rates Also the ultrafiltration capacity of the devices was determined It was found that a reasonable estimation of the ultrafiltration capacity could be made The calculated clearance rates were systematically underestimated, although the relative dependence of the clearance rates on the applied sterilization methods was approximated reasonably

Keywords artificial kidney, dialysis, including Donnan, membrane preparation and structure, membrane characterization, thermoporometry

Introduction

Hollow fiber cellulosic membranes are now used for more than two decades in artificial kidneys, in which they act as a separation barrier for metabolic wastes The apparent performance of an artificial kidney device is not only a function of membrane permeability One should realize that disturbing effects like concentration polarization and membrane fouling are all induced by the existence of the membrane wall and therefore by its characteristic structure Detailed knowledge on membrane structure parameters and how these depend on the production process can help the manufacturer to

Correspondence to Arnold P Broek, University of Twente, Dept of Chemical Technology, P O Box 217, 7500 AE Enschede (Netherlands) Phone X-31 53 89 3474, fax X-31 53 356024

*Paper presented at the Int Symp "Progress in Membrane Science and Technology", Enschede, Netherlands, June 25–28, 1991

**Present address Organon Teknika B V , P O Box 84, 5280 AB Boxtel (Netherlands)

choose optimal conditions Characterization of the structure of membranes however is a difficult task This is partly due to the many types of membranes and membrane processes that exist and partly due to the typical characteristics of membranes and the sometimes vague definition of the parameters which are determined [1]

Cellulosic dialysis membranes often are considered to be hydrogels The morphology and mass transport characteristics of these membranes are strongly dependent on the extent of swelling For hydrogels it has been proposed that at least two types of water can be distinguished, namely 'bound' water and 'bulk-like' water [2]. Bound water is strongly associated with the polymer matrix and therefore not undergoing phase transition when cooled to temperatures far below the normal freezing point of water Several authors [3,4] tried to elucidate the role of both types of water in mass transport through hydrogels

From the above it is clear that for an appropriate determination of membrane morphology parameters like pore size (distribution), porosity and membrane thickness conditions close to the membrane operating conditions are essential For hemodialysis membranes this means that the membranes have to be examined in the water swollen state Furthermore, pore sizes of these membranes typically are in the range of a few nanometers which means that only a limited number of available characterization techniques can be applied

An indirect method to characterize the morphology of hemodialysis membranes was proposed by Klein et al [5] By fitting diffusive solute and pure water permeability data to a capillary pore model they could obtain values for the surface porosity and an average effective pore radius for several membrane types The method was extended by Sakai et al. who introduced a tortuosity factor in the model [6] Although the results were found to be slightly dependent on the solutes used, consistent results could be obtained Typical values found for Cuprophan dialysis membranes were an effective pore radius of 2–3 nm, a surface porosity of 30% and a tortuosity factor of 2

Hanemaayer et al [7] estimated the pore sizes of different flat sheet membranes from rejection measurements with oligo-saccharides For a low cut-off regenerated cellulose membrane they reported a pore radius of 2 3–3 nm

It should be emphasized that the parameters obtained are the result of fitting experimental results to a simplified cylindrical pore model and that therefore the results do not necessarily correspond with reality For example, Yasuda and Lamaze [8] reported that for the same Cuprophan membrane a sieving effect was absent for molecules as large as bovine serum albumine (BSA) It is hard to imagine that BSA molecules could permeate through pores of the mentioned dimensions without any significant sieving effect Furthermore it is reasonable to assume that in reality a distribution of pore sizes exists in the membrane Regarding this fact it is difficult to hold the concept of an average or effective pore size because this value must be dependent on the solute or solvent that is permeating Large molecules can only permeate through the larger pores of the membranes while small molecules can permeate through both the small and the large pores Small pores do not contribute to the transport of large molecules which means that the effective pore size obtained from permeation experiments must depend on the dimensions of the permeant Analogous arguments can be given for the porosity and tortuosity factor

Recently Tatsuguchi and Sakai [9] reported on the determination of pore sizes of regenerated celluloses from the lowering of the melting-point of ice in the pores of the membranes. However, unfortunately their results where interpreted assuming an uniform pore size The reported pore radii were between 2 5 and 3 nm

Thermoporometry is a relatively new characterization technique to determine the pore size distribution and porosity of meso-porous materials (2–50 nm) The method, developed by Brun et al [10], is based on the calorimetric analysis of the liquid–solid transformation in liquid filled porous materials It is a wet-state characterization technique which can therefore be helpful in the characterization of water swollen hemodialysis membranes made from regenerated celluloses.

In this work we report on our research concerning the effect of two commonly used sterilization methods for artificial kidneys on the morphology and performance of Hemophan® hemodialysis membranes. As was shown by several authors [11–14] sterilization or other treatments can have a dramatic effect on the structure and performance of cellulosic membranes

Theoretical

Thermoporometry

Thermoporometry is based on the observation that the equilibrium condition of the solid, liquid and gaseous phase of a highly dispersed pure substance is determined by the curvature of the interface In a liquid filled porous material, e g a membrane, the solidification temperature of the liquid depends on the liquid–solid interface in the pore The minimal size of a stable crystal (R_c) is inversely proportional to the degree of undercooling and in the finely porous material the liquid therefore crystallizes or melts at the temperature where the pore radius R_p equals R_c The melting or solidification thermogram can be monitored in a differential scanning calorimeter (DSC) and translated to a pore size When the membrane is heteroporous, a pore size distribution is obtained A schematic representation of the endothermic heat effect measured from the melting of a liquid in a porous medium is shown in Fig 1

Brun et al [10] derived simple equations relating R_p and the apparent transition heat effect W_a of several pure substances with the extent of undercooling $\Delta T = T - T_o$, where T_o is the normal phase transition temperature of a liquid (0 °C for water) and T is the temperature where the phase transition is actually observed when this liquid is contained in pores For cylindrical pores filled with melting ice Brun derived the following equations:

$$R_p = \frac{-32\,33}{\Delta T} + 0\,68 \qquad (1)$$

$$W_a = -0\,155\Delta T^2 - 11.39\Delta T - 332 \qquad (2)$$

Equations (1) and (2) are slightly different for the case of pores filled with freezing water. Brun also derived analogues relations for a spherical pore geometry Although Hemophan is unlikely to contain regular cylindrical or spherical pores, for the sake of comparison the cylindrical pore model was assumed

The shaded area under the curve (Fig 1) between T and $T+dT$ represents the heat effect of the melting of ice in pores with radii in the range between R_p and R_p+dR_p, given by eqn (1) From the heat effect (in Joule) the pore

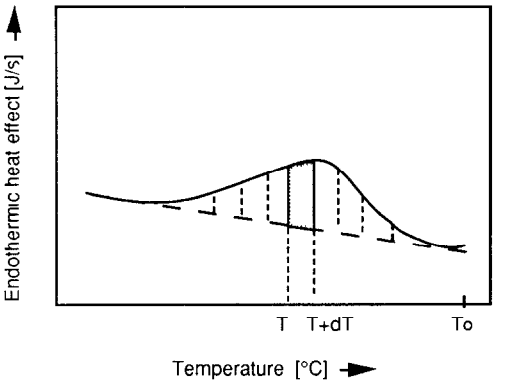

Fig 1 Schematic representation of the endothermic heat effect from the melting of a liquid in a porous medium as a function of temperature

volume of the pores with radii between R_p and $R_p + dR_p$ can be calculated with the help of eqn (2) Pore volume distributions are presented as dV/dR_p as a function of R_p. The quantity dV/dR_p is given by the amount of pore volume dV (per gram of dry membrane material) measured in a certain pore size interval divided by the size of that interval The total amount of pore volume per gram of swollen membrane material can be obtained from a summation of the pore volumes measured for every temperature interval $T + dT$.

Performance

Artificial kidney performance is often expressed in a so called clearance rate and the ultrafiltration capacity (UFR). The clearance rate is the volume which is cleared of a certain substance per unit of time The clearance rate is determined from an experiment with a negligible pressure difference, according to eqn. (3)

$$Q_{cl} = Q_b \frac{c_{b,in} - c_{b,out}}{c_{b,in}} \tag{3}$$

For a pure counter-current configuration the relation between clearance rate Q_{cl} and solute permeability P is given by eqn (4) [15]

$$Q_{cl} = \frac{Q_b Q_d \left[1 - \exp\left(\frac{-PA(Q_d - Q_b)}{Q_d Q_b} \right) \right]}{Q_d - Q_b \exp\left(\frac{-PA(Q_d - Q_b)}{Q_d Q_b} \right)} \tag{4}$$

where A is the logarithmic mean surface area·

$$A = NL\pi \frac{d_o - d_i}{\ln(d_o/d_i)}$$

The solute permeability P in eqn. (4) is an overall permeability which is related to the solute permeability of the membrane according to eqn (5)

$$\frac{1}{P} = \frac{1}{P_m} + \frac{1}{P_b} + \frac{1}{P_d} \tag{5}$$

The permeability of the boundary layer in the fiber lumen can be estimated from eqn (6) [11]:

$$P_b = \frac{4D}{d_i} \tag{6}$$

The permeability of the boundary layer in the shell side of the device can be estimated from relations proposed by Sigdell [15] Although, because of its length, the relation is not given here its appearance is comparable with eqn (6). Especially at the shell side of hollow fiber devices very accurate estimations of the influence of boundary layers are hardly possible because the streaming conditions are not well known The influence of boundary layers on overall membrane permeability is most important for low molecular weight solutes [16] According to the tortuous capillary pore model [6] the solute and pure water permeabilities can be expressed by eqns (7) and (8)

$$P_m = \frac{A_k f(q) S_d(q) D}{\tau \Delta x} \tag{7}$$

$$L_p = \frac{A_k R_p^2}{8\eta\tau\Delta x} \tag{8}$$

where·

$$f(q) = (1 - 2.1q + 2.1q^3 - 1.7q^5 + 0.72q^6) / (1 - 0.76q^5)$$

$$S_d(q) = (1-q)^2$$

$$q = \frac{R_s}{R_p}$$

Equation (7) is based on an equation originally derived by Verniory et al. [17] for neutral spherical solute molecules diffusing through a cylindrical pore Equation (8) is a modification of the Hagen–Poiseuille equation. Klein et al [5] and Sakai et al [6] used these same equa-

tions to evaluate the morphology of their membranes.

From thermoporometry a pore size distribution and a volume porosity ϵ are obtained Equations (7) and (8) can be rewritten as follows

$$P_m = \frac{\sum_{i=1}^{n} \epsilon_i f(q_i) S_d(q_i) D}{\tau^2 \Delta x} \quad (9)$$

$$L_p = \frac{\sum_{i=1}^{n} \epsilon_i R_{p,i}^2}{8\eta\tau^2 \Delta x} \quad (10)$$

where $\epsilon = A_k \tau$

Experimental

Materials

For the experiments artificial kidney devices filled with 8 μm wall thickness Hemophan® were used The devices were provided by Organon Teknika, all membrane material was originating from the same production batch Three differently treated devices were examined, namely non-sterilized, ethylene oxide (EtO) sterilized and steam sterilized. Technical data are given in Table 1. The steam sterilized membrane samples used for this study were sterilized in the dry state and not treated with a concentrated glycerol solution before sterilization Normally artificial kidney manufacturers steam sterilize their Cuprophan and Hemophan membranes either in the water swollen state or after a treatment with a concentrated glycerol solution Both methods prevent the membrane from a dramatic change in structure and performance [18] Therefore the steam sterilized samples used in this study are not comparable with commercially available steam sterilized Hemophan or Cuprophan membranes

TABLE 1

Technical data of the artificial kidney devices (data provided by Organon Teknika)

Membrane material	Hemophan®
Wet inner fiber diameter	214 μm
Wet membrane wall thickness	21 5 μm
Wet surface area	0 888 m^2
Fiber length	0 225 m
Number of fibers	5350

Changes in membrane dimensions due to the applied sterilization procedures were ignored. All water used for this study was demineralized and ultrafiltrated All chemicals were of pro analysis quality Stokes radius and diffusivity of the solutes at 310 K are [5]·

Creatinine

$R_s = 0\ 246$ nm, $D = 1\ 29 \times 10^{-9}$ m^2-sec^{-1}

Vitamin B12:

$R_s = 0\ 836$ nm, $D = 0.379 \times 10^{-9}$ m^2-sec^{-1}.

Water viscosity at 310 K is

6.95×10^{-4} Pa-sec [19].

Performance

In vitro clearance rate measurements were carried out with creatinine and vitamin B12. Diluted solutions of the solutes were pumped through the lumen side of the devices with a flow rate of 200 ml/min Water was pumped through the shell side with a flow of 500 ml/min. Both flow rates were single pass. The trans membrane pressure (TMP) was kept minimal (50 mbar) during the experiments. Concentrations of creatinine and vitamin B12 were determined spectrophotometrically at 234 and 550 nm respectively with a Phillips PU8720 spectrophotometer The ultrafiltration capacity was determined from the clean water flux at a TMP of 200 mbar The TMP is defined as

$$TMP = \frac{p_{b,in} + p_{b,out}}{2} - \frac{p_{d,in} + p_{d,out}}{2}$$

Thermoporometry

Samples were prepared by cutting the dry hollow fibers in pieces of about 6 cm The material was swollen in water (containing 200 mg/l formaldehyde) which was refreshed several times About 16 mg of swollen material was securely wiped with tissues to remove the water from the fiber lumen as much as possible and then frozen with maximal speed (ca. 320°C/min) to a temperature of −40°C in the DSC-apparatus The thermogram was obtained by subsequently heating the sample with a speed of 1°C/min to +10°C

The experiments were carried out with a Perkin-Elmer DSC-IV equipped with a data processing unit, the final thermograms (containing about 600 data points) were transferred to a spread sheet program for further calculations In general the obtained thermograms showed no curvature of the base line and therefore a linear base line was chosen between −35°C and +10°C. Peak integration was done numerically using Simpson's rule

Swelling values of the membranes were determined from the weight decrease upon drying about 100 mg sample (after wiping) in a vacuum oven at 80°C The swelling value was used to calculate the dry weight of each swollen sample used in the DSC-measurements

Results and discussion

In Fig 2 a typical thermogram is shown Two separate peaks can be distinguished Peak 1 represents the melting of ice in the pores of the membrane Peak 2, which starts at approximately 0°C is due to the melting of ice which is not in the pores but adhering to the membrane wall or in the fiber lumen

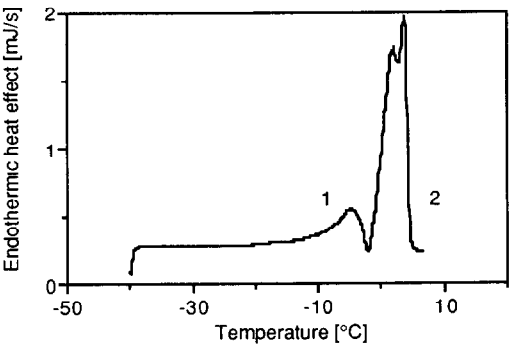

Fig 2 Typical thermogram of an Hemophan dialysis membrane

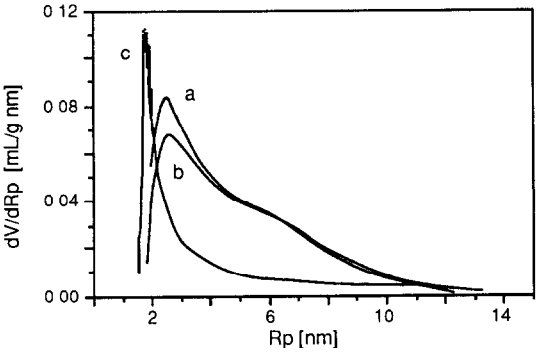

Fig 3 Differential pore volume distributions of the differently treated Hemophan samples (a) Non-sterilized, (b) EtO sterilized, (c) steam sterilized

In Fig 3 the average pore volume distribution curves are shown, experiments were performed in duplo From the figure it can be seen that Hemophan membranes contain pores with radii between 1 5 and 12 nm. The curves of the non-sterilized and EtO sterilized sample have their maximum (R_{max}) at 2 5 nm, R_{max} corresponds with the pore class that has the largest contribution to the overall pore volume The value for R_{max} is in the range of pore radii that were reported by Tatsugushi and Sakai [9] Due to the steam sterilization treatment R_{max} shifts to a lower value of 1 6 nm

In Table 2 the calculated mass fractions of pore water in the swollen membranes are given The values are corrected for the amount of

TABLE 2

Mass fraction of pore water and estimated values for the volume fraction of pore water, non-freezing water and polymer

Sterilization	Mass fraction of pore water	ϵ (v/v)	V_{nf} (v/v)	V_{pol} (v/v)
Non	0 165	0 204	0 350	0 446
EtO	0 147	0 182	0 354	0 464
Steam	0 081	0 103	0 366	0 531

water that was found in peak 2 of the thermogram EtO sterilization yields a somewhat lower porosity compared to the non-sterilized device From Fig 3 it can be seen that this decrease is the result of a partial collapse of the smallest pores (2–4 nm), the pore volume of the larger pores seems constant Steam sterilization of Hemophan results in a drastically lower porosity. It appears that the number of larger pores has decreased while the number of the smallest pores has increased. This observation suggests that the crosslink density of the polymer network has been increased The swollen steam sterilized membrane samples clearly had a light brown colour indicating that chemical reactions had occurred

The fractions of pore water calculated from the plots in Fig 3 are mass fractions For mass transport calculations the volume fraction of pore water in the membrane is needed Direct determination of this value is difficult for hollow fibers. Furthermore the volume fraction of water is not equal to the volume fraction of pores found with thermoporometry because a substantial part of the available water is present as bound water In Table 2 estimations for the volume fractions of pore water, bound water and polymer are given The calculations are based on the measured thermograms assuming that the specific densities of water and cellulose are 1000 and 1520 kg/m^3 [20] respectively The amount of bound water is calculated from the difference between the total amount of water in the sample (calculated from the weight decrease upon drying the sample in a vacuum oven at 80°C) and the amount of water found in peak 1 and 2 of the thermogram Because bound water is not undergoing phase transition it can not be detected directly in a DSC The sum of the volume fractions of pore and bound water is equal to the total volume fraction of water in the membrane

From Table 2 it can be seen that the total volume fraction of water in the membrane is decreased due to the sterilization treatments The differences in volume fraction water in the samples are due to the different fractions of pore water in the samples

Table 3 shows the results of the performance measurements The effect of EtO sterilization on the performance is relatively small The effect of steam sterilization is much more drastic, especially for the vitamin B12 clearance rate and the UFR This also indicates that the steam sterilization treatment mainly decreases the number of large pores as was already shown in Fig 2

Using eqns (4)–(6) and (9) and (10) it is possible to calculate an estimation of the performance of the artificial kidneys on the basis of the measured pore size distributions The only unknown factor in eqns (9) and (10) is the tortuosity factor which has to be estimated For the calculations it was assumed that the tortuosity was 1 9, a value reported by Sakai et al [6] Results of the calculations are given in Table 4

TABLE 3

Measured performance values ($n=3$)

Sterilization	Clearance rate (ml/min)		UFR (ml/hr)
	Creatinine	Vitamin B12	
Non	145±6	43±3	725± 3
EtO	142±4	41±1	680± 6
Steam	66±3	5±2	77±10

TABLE 4

Calculated performance values

Sterilization	Clearance rate (ml/min)		UFR (ml/hr)
	Creatinine	Vitamin B12	
Non	83	18	759-976
EtO	78	17	735
Steam	44	4	90

It appears from Tables 3 and 4 that the UF-capacities are predicted rather well, the estimated values are 10 to 20% higher than the measured ones The clearance rate values however are systematically underestimated, although the relative dependence of the clearance rate on the applied sterilization method is approximately reasonably The calculated clearance rates are 40–60% too low. For the calculations it was assumed that only the pore water found from the thermoporometry experiments was contributing to the mass transport properties of the membrane The bound water was considered as inert membrane material. From Table 2 it is clear that the major part of the water in the membranes is bound water On the other hand Klein and Sakai assumed for their calculations that the pore volume was approximately equal to the volume of water in the polymer, and that as a consequence all membrane water was contributing to mass transport The reported surface porosities are larger than the volume porosities reported in Table 2. Furthermore the effective pore radii that were reported by Klein and Sakai are very near to the minimal pore sizes that were found with thermoporometry, which means that a relatively high surface porosity was needed to fit the experimental results

Assuming that the low calculated clearance rates are only caused by underestimated values for the membrane permeability (and not by boundary layer permeabilities etc) it can be calculated how large these underestimations of P_m are For example for the clearance rates of the non-sterilized samples both the creatinine and vitamin B12 clearance rate are underestimated with approximately 72% From Table 2 it can be calculated that the amount of pore volume for these membranes is only 35% of the total water volume Then if we assume that all water in the membrane is accessible for mass transport and that any sieving effect is absent $[f(q)S_d(q)=1]$, the calculated creatinine and vitamin B12 clearance rate would be 144 and 69 respectively The recalculated clearance rate value for creatinine is very close to the measured value, while for the larger molecule vitamin B12 the clearance rate now is overestimated Apparently for a small molecule like creatinine both the bound and the pore water of this membrane are accessible, while for the larger molecule of vitamin B12 only a fraction of the total water is accessible.

Conclusions

It is concluded that thermoporometry provides a strong tool for studying changes in pore morphology of Hemophan hemodialysis membranes Data obtained from this technique can be used to predict membrane performance

List of symbols

A	logarithmic mean surface area (m^2)
A_k	surface porosity (-)
c_b, c_d	concentrations in lumen and shell side of the device ($mol\text{-}m^{-3}$)
D	solute diffusivity in water ($m^2\text{-}sec^{-1}$)
d_i, d_o	wet inner and outer fiber diameter (m)
$f(q)$	wall correction factor for diffusion (-)
L	effective fiber length (m)
L_p	pure water permeability ($m^3\text{-}m^{-2}\text{-}Pa^{-1}\text{-}sec^{-1}$)
N	number of fibers in the device (-)

P	overall solute permeability (m-sec^{-1})
P_b	permeability boundary layer lumen side of the device (m-sec^{-1})
P_d	permeability boundary layer shell side of the device (m-sec^{-1})
P_m	membrane permeability (m-sec^{-1})
p_b, p_d	pressure at lumen and shell side of the device (Pa)
q	R_s/R_p (-)
Q_b	flow rate through lumen side of the device (m^3-sec^{-1})
Q_{cl}	solute clearance rate (m^3-sec^{-1})
Q_d	flow rate through shell side of the device (m^3-sec^{-1})
R_c	minimal radius of a stable crystal (nm)
R_p	pore radius (nm)
R_s	Stokes radius of solute (nm)
$S_d(q)$	steric hindrance factor for diffusion (-)
T	temperature at which phase transition occurs (°C)
T_o	normal phase transition temperature of the liquid (°C)
ΔT	$= T - T_o$ extent of undercooling (°C)
TMP	trans membrane pressure (Pa)
UFR	ultrafiltration capacity (m^3-sec^{-1})
V_{nf}	volume fraction non-freezing or bound water (-)
V_{pol}	volume fraction polymer (-)
W_a	apparent transition heat effect (J-g^{-1})
Δx	membrane wall thickness (m)
ϵ	volume porosity (-)
η	viscosity (Pa-sec)
ρ	density (kg-m^{-3})
τ	tortuosity factor (-)

References

1 F P Cuperus and C A Smolders, Characterization of UF membranes Membrane characteristics and characterization techniques, Adv Colloid Interface Sci , 34 (1991) 135-172

2 A Higuchi, J Komiyama and T Iijima, The states of water in gel cellophane membranes, Polym Bull , 11 (1984) 203-208

3 S W Kim, J R Cardinal, S Wisniewski and G M Zentner, Solute permeation through hydrogel membranes, in S P Rowland (Ed), Water in Polymers, ACS Symp Ser , No 127 American Chemical Society, Washington, DC, 1980, 347-359

4 Z Morita, H Ishida, H Shimamoto, R Weber and P Rys, Anion permeability of cellulosic membranes Part I Porosity of water-swollen membranes, J Membrane Sci , 46 (1989) 283-298

5 E Klein, F F Holland and K Eberle, Comparison of experimental and calculated permeability and rejection coefficients for hemodialysis membranes, J Membrane Sci , 5 (1979) 173-188

6 K Sakai, S Takesawa, R Mimura and H Ohashi, Structural analysis of hollow fiber dialysis membranes for clinical use, J Chem Eng Jpn , 20 (1987) 351-356

7 J H Hanemaaijer, T Robbertsen, Th van de Boomgaard, C Olieman, P Both and D G Schmidt, Characterization of clean and fouled ultrafiltration membranes, Desalination, 68 (1988) 93-108

8 H Yasuda and C E Lamaze, Permselectivity of solutes in homogeneous water-swollen polymer membranes, J Macromol Sci Phys , B5(1) (1971) 111-134

9 T Tatsuguchi and K Sakai, Determination of structure and permeability of drawn hollow fiber dialysis membranes of regenerated cellulose, Ext Abstr ICOM'90, Chicago, USA, 1990, N N Li (Ed), NAMS, pp 1238-1239

10 M Brun, A Lallemand, J F Quinson and C Eyraud, A new method for the simultaneous determination of the size and the shape of pores thermoporometry, Thermochim Acta, 21 (1977) 59-88

11 E Klein, F F Holland, A Donnaud, A Lebeouf and K Eberle, Diffusive and hydraulic permeabilities of commercially available cellulosic hemodialysis films and hollow fibers, J Membrane Sci , 2 (1977) 349-364

12 S Takesawa, S Ohmi, Y Konno, M Sekiguchi, S Shitaokoshi, T Takahashi, H Hidai and K Sakai, Varying methods of sterilization, and their effects on the structure and permeability of dialysis membranes, Nephrol Dial Transplant , 1 (1987) 254-257

13 S Takesawa, S Satoh, H Hidai, M Sekiguchi and K Sakai, Degradation by gamma irradiation of regenerated cellulose membranes for clinical dialysis, Trans Am Soc Artif Intern Organs, 33 (1987) 584-587

14 A P Broek, D Bargeman, E D Sprengers and C A Smolders, Characterization of hemophan hemodialysis membranes by thermoporometry, Int J Artif Organs, 15 (1992) 25-28

15 J E Sigdell, Calculation of combined diffusive and convective mass transfer, Int J Artif Organs, 5(6) (1982) 361-372
16 C K Colton and E G Lowrie, Hemodialysis Physical principles and technical considerations, in B M Brenner and F C Rector (Eds), The Kidney, Vol II, 2nd edn , Saunders, Philadelphia, 1981, p 2425
17 A Verniory, R Dubois, P Decoodt, J P Gassee and P P Lambert, Measurement of the permeability of biological membranes, J Gen Physiol , 62 (1973) 489
18 Sterilization of Cuprophan and Hemophan, Enka AG, Product Group Membrana, Wuppertal, Germany, 1986
19 R C Weast (Ed), Handbook of Chemistry and Physics, Chemical Rubber Co , Cleveland, OH, 52nd edn , 1971
20 C K Colton, K A Smith, E W Merrill and P C Farrell, Permeability studies with cellulosic membranes, J Biomed Mater Res , 5 (1971) 459-488